LA-UR- 97-4334

Title: ANALOG NEURAL NETWORK CONTROL METHOD PROPOSED FOR USE IN A BACKUP SATELLITE CONTROL MODE

CONF-971086--

Author(s): Janette R. Frigo
Mark W. Tilden

Submitted to: SPIE - INTELLIGENT SYSTEMS & ADVANCED MANUFACTURING
October 14-17, 1997
Pittsburg, Pennsylvania

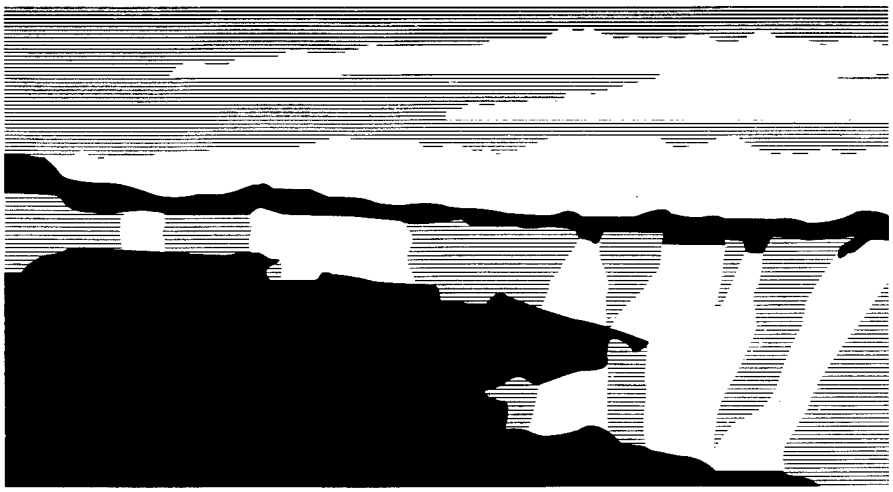

Los Alamos
NATIONAL LABORATORY

Form No. 836 R5
ST 2629 10/91

DISCLAIMER

Analog neural network control method proposed for use in a backup satellite control mode

Janette R. Frigo, Mark W. Tilden

Los Alamos National Laboratory, MSD466/NIS-1, Los Alamos, NM, 87545

ABSTRACT

We propose to use an analog neural network controller implemented in hardware, independent of the active control system, for use in a satellite backup control mode. The controller uses coarse sun sensor inputs. The field-of-view of the sensors activate the neural controller, creating an analog dead band with respect to the direction of the sun on each axis. This network controls the orientation of the vehicle toward the sunlight to ensure adequate power for the system. The attitude of the spacecraft is stabilized with respect to the ambient magnetic field on orbit. This paper develops a model of the controller using real-time coarse sun sensor data and a dynamic model of a prototype system based on a satellite system. The simulation results and the feasibility of this control method for use in a satellite backup control mode are discussed.

Keywords: analog neural network, autonomous control mode, satellite systems

1. INTRODUCTION

A space environment requires that the spacecraft (SC) systems conserve power, be reliable, and self-contained while being able to withstand severe environmental specifications. Over the past fifty years there have been dramatic improvements in methods of designing spacecraft systems, however, every conceivable failure-mode cannot be predicted. Control systems must adapt to failures. For example, the Department of Energy's (DOE) ALEXIS spacecraft experienced structural damage during launch which caused orientation problems and loss of subsequent communications for part of the mission[1]. The ALEXIS control system has not functioned autonomously after this failure. Currently, all control operations for ALEXIS are sent up from the ground station.

Satellite systems employ various control modes such as vehicle acquisition, vehicle position (i.e. attitude control), and backup control modes. The backup mode, in particular, for satellite systems of the future (e.g. Iridium, a constellation of 66 satellites intended for global communications) requires an autonomous scheme. One such method relies on filtering data from a three axis magnetometer[2] to estimate position and velocity. The equations of motion are used to propagate these estimates. This method uses a Kalman filter algorithm on three-axis magnetometer data and works independently of attitude control knowledge. Therefore, it a possible choice for use as a backup control mode during operational anomalies. Other methods of autonomous navigation rely on observations of celestial bodies or observations of landmarks on the Earth. A technique that relies on sensing the Sun, the Earth and the moon[3] could be useful on low-Earth-orbit vehicles where mission requirements allow low accuracy but demand autonomy. The Global Positioning System (GPS) can be used for autonomous navigation if the satellite has an on-board GPS receiver. On the FORTE satellite, if either the horizon sensor or the scanwheel fails at any point during the mission, a backup control mode can be accommodated via a passive stabilization method.[4] However,

knowledge of the satellite attitude is necessary. All of these methods rely on prediction algorithms and data from on-board sensors or receivers, and thereby, are somewhat semi-autonomous.

An analog neural network controller is investigated that locates the autonomy of the control system in the hardware, maintaining proper positioning for solar and mission requirements. In the first section, the network structure used in the proposed autonomous system is explained. The controller uses coarse sun sensor inputs and the field-of-view of the sensors to activate the neural controller, creating an analog dead band with respect to the direction of the sun on each axis. The neural network controls the orientation of the SC vehicle toward the sunlight to ensure adequate power for the spacecraft system. The mathematical model for the proposed system is derived in section 4. The subsystem modules consist of the controller, the sensor inputs, the actuator, and the plant dynamics. Next, spacecraft control systems for attitude control and backup control modes are described. The SIMULINK results for angular position based on sensory input are discussed. The results of the closed-loop (SIMULINK) simulation are compared to typical specifications for a backup control mode on a low earth orbit satellite[4].

2. NEURAL NETWORK

2.0 Neural network structure

The neuron is a digital summing differentiator neuron which determines the triggering and time delay of signals (or processes) through the network[6]. The input delay to the neuron is set by the sum of the external bias inputs. In this case, it is a high pass delay. Based on the inner threshold level, the output changes state. The inverting buffer-driver (a Schmidt trigger) is a comparator with hysteresis. The input delay, modulated via sensor activation, decreases the time constant of the neuron and the current across the output load. In this context, the neuron is referred to as *inhibitory*.

The network is a directed loop of two or more neurons connected in series, that is, the output of one neuron is connected to the input of the preceding neuron, and so forth. This neuron network is shown in Fig. 1. The frequency of oscillation for the individual neurons is modulated from the analog sensor input. Sensor activation decreases the high pass time constant of the activated neuron so the on-time duty cycle is decreased. This difference causes more power to be delivered in the opposite direction of sensor activation, and produces a torque in the direction of the light source. The activation can be varied, but as long as one sensor is activated more than the other, the motion will be directed toward the sensor with greatest activation. In the same way, the sensors could be reversed to cause motion away from the light if desired.[7]

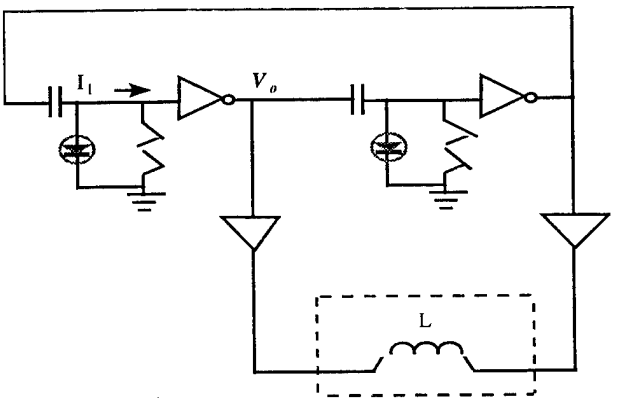

Fig. 1. Two neuron network system.

3. CONTROL SYSTEM MODEL

In this section, a model for the proposed system is derived. The equations to describe the neuron controller, the actuator, and the set of equations of motion for the plant dynamics of this system are developed. The sensor input to the controller is real-time coarse sun sensor data from the ALEXIS satellite.

3.1 Neural network controller

The equations for modeling the input characteristic for the neuron are the KVL equation to describe the voltage across the high pass RC input,

$$V_1 = I_1 R + \frac{1}{C}\int I_1 dx \tag{1}$$

where C is the capacitance and R is the parallel combination of a constant stabilizing resistance and ΔR, the sensor input data. The next component is the inverting input buffer, a bistable comparator with hysteresis. This is modeled as,

$$V_o(t) = \begin{cases} 5v & V_1 \le 1.9v \\ 0v & 1.9v \le V_1 \le 2.9v \end{cases} \tag{2}$$

where I_1, V_1 are the input current and voltage and V_o is the output voltage from the neuron. A saturation function for negative voltage is placed at the input to this function since the buffer is reverse voltage protected. The neural network consist of two neurons connected in series, that is, the input of one neuron is connected to the output from the preceding neuron, and so forth. In this way, the oscillator changes state according to the high pass RC delay and the trigger levels of the buffer (schmidt trigger). The SIMULINK model of the neuron is given in Appendix A, Fig. A1.

In order to improve the closed loop stability characteristics, a phase-lead filter is designed at the input to the sensors. This filters the position error, adding positive phase to the system over the appropriate frequency range. The transfer function for this network in terms of voltage is

$$\frac{V_2}{V_1} = \frac{R_2 + R_1 R_2 C s}{R_1 + R_2 + R_1 R_2 C s}. \tag{3}$$

3.2 Sensor model

Sun sensors are among the most widely used sensor types on orbital vehicles. The angular radius of the Sun is independent of SC orbit and sufficiently small[8], so most applications use a point-source approximation for determination. In this case, both sensor design and the attitude determination method are simplified as the Sun is sufficiently bright such that low power, simple, reliable technology can be used without discriminating among sources of light. The Sun is distinguishable from other sources of light. Many missions have Sun-related thermal constraints, and nearly all require the Sun for power. Sun sensors are used to protect sensitive equipment such as star trackers, to provide a reference for onboard attitude control, and to position solar power arrays. As a result of their multiple functions, sensors vary appreciably with respect to their field of views (FOV) and resolutions.

The analog sensors called cosine detectors have a continuous monatomic output signal from a sinusoidal variation of the output current of a silicon solar cell with respect to the Sun angle. Therefore, the output current, I, is proportional to the cosine of the angle of incidence of the solar radiation. The simplified model for current is,

$$I(\theta) = I(0)\cos\theta\,. \tag{4}$$

Sensors of this type are used as course Sun detectors on many SC missions such as ALEXIS.[9] Apertures are used to limit the FOV of an analog sensor. A group of cosine detectors, each with a limited FOV, can provide intermediate accuracy over a wide angular range.

In this proposed scheme, the FOV and the location of the analog sensors detect the light intensity and produce an output signal that is a continuous, monatomic function of solar intensity. In one scenario, the controller is off when the sensor is within the FOV of the sun and starts oscillating when it falls out of view of the sun or vise versa. The results of sensor activation for an axis which demonstrates phototropic motion is given in section 5.

3.3 Actuator model

The neural controller supplies current to the actuator in alternating directions based on the frequency of oscillation of the network. For simplicity, a single air-core inductor is modeled. The inductor is pulsed with current to create a magnetic field which reacts with the local magnetic flux density on orbit. The torque is directly related to the current supplied to the actuator, geometry of the coil, and sensor activation (neuron frequency). The equation to describe the magnetic dipole moment of an air-core torque coil is,

$$\mathrm{m}_{\mathrm{o}} = \mathrm{INA}\hat{\mathbf{s}} \tag{5}$$

where **s** is a unit vector normal to the plane of the coil. The maximum magnetic moment is m_{o}, N is the number of turns for a coil, A is the enclosed area of the current loop, and I is the current through the loop. The equation to describe the current across the inductor is,

$$\frac{d\mathrm{I}}{dt} = \frac{\mathrm{V}_L}{\mathrm{L}} + \frac{\mathrm{IR}_L}{\mathrm{L}}\,. \tag{6}$$

V_L is the voltage across the inductor and the impedance is $\mathrm{Z} = \mathrm{R}_L + \omega L$. The actuators are determined by the mission requirements and the SC control system hardware design. Magnetic torque coils are frequently used on low-earth orbit spacecraft missions where the earth's magnetic field is sufficiently strong.

3.4 System dynamics model

Free-body (i.e. satellite) motion differs in several important respects from the motion of rigid objects supported in a gravitational field. A rigid body is a dynamical system with three degrees of freedom associated with the translational motion of a given point in the body, typically the center of mass, and three degrees of freedom describe the rotational motion. The equations of motion for the translational degrees of freedom are the equations of motion for a mass particle and are easily determined. Thus, the equations of motion for the rotational degrees of freedom are developed.

3.4.1 Angular momentum and moment of inertia tensor

In rotational dynamics the angular momentum, **L**, is defined as,

$$\mathbf{L} = \mathbf{I}\omega\,. \tag{7}$$

The quantity **I** is called a tensor because it has specific transformation properties under a real orthogonal transformation. It is a real symmetric 3x3 matrix, thus, it has three real orthogonal eigenvectors and three eigenvalues. The scalers I_i, for i = 1, 2, 3

are the principal moments of inertia, and the unit vectors, are the principle axes. If the principle axis is used as the coordinate axis of a spacecraft reference frame, the moment of inertia tensor takes the diagonal form,

$$\mathbf{I} = \begin{bmatrix} I_1 & 0 & 0 \\ 0 & I_2 & 0 \\ 0 & 0 & I_3 \end{bmatrix} \tag{8}$$

Thus, the principle axis can be thought of intuitively as axis around which the mass is symmetrically distributed. Any axis of rotational symmetry of the mass distribution is a principal axis.

3.4.2 Euler's Equations of rotational motion

The basic equation of attitude dynamics relates the time derivative of the angular momentum vector to the applied torque, **N**. This relation is the time derivatives of the components of **L** along the spacecraft-fixed axes because the moment of inertia tensor of a rigid body is a constant. The equation for the time derivative of the angular momentum vector is

$$\frac{d\mathbf{L}}{dt} = \mathbf{N} - \omega \times \mathbf{L} = \mathbf{I}\frac{d\omega}{dt} \tag{9}$$

where the torque vector is **N** and ω is the instantaneous angular velocity. In the case of spacecraft applications, internal torques cancel and the net torque, **N**, is due to external forces. The above equation is the fundamental equation of rigid body dynamics. The presence of $\omega \times \mathbf{L}$, means that **L** and ω are not constant in the spacecraft frame. The resulting motion is called *nutation*. Rotational motion without nutation occurs only if ω and **L** are parallel, that is, only if the rotation is about the principle axis of the rigid body. The latter case is modeled (Appendix A, Fig. A4) since rotation is about the principle axis of the rigid body for the prototype system.

Equation (9) can be expressed as

$$\mathbf{I}\frac{d\omega}{dt} = \mathbf{N} - \omega \times (\mathbf{I}\omega) \tag{10}$$

and the vector quantities in the principle axis coordinate form are

$$\begin{aligned} I_1 \frac{d\omega_1}{dt} &= N_1 + (I_2 - I_3)\omega_2\omega_3 \\ I_2 \frac{d\omega_2}{dt} &= N_2 + (I_3 - I_1)\omega_3\omega_1 \\ I_3 \frac{d\omega_3}{dt} &= N_3 + (I_1 - I_2)\omega_1\omega_2 \end{aligned} \tag{11}$$

These are Euler's equations. They are three coupled, nonlinear, first order differential equations which constitute one-half of the equations of motion for a rigid body. Since Euler's equations will supply us with the three components of the angular velocity vector, ω, in the body frame, the other three equations can be found by expressing the angular velocity in terms of the Euler angles, θ, ψ, and ϕ. In terms of the body frame unit vectors, the angular velocity vector, ω, can be expressed in body frame components as

$$\begin{aligned} \omega_1 &= \theta\cos(\phi) + \varphi\sin(\theta)\sin(\phi) \\ \omega_2 &= \theta\sin(\phi) - \varphi\sin(\theta)\cos(\phi) \\ \omega_3 &= \varphi\cos(\phi) + \phi \end{aligned} \tag{12}$$

for a particular rotation sequence.[10] The set of equations in eqn. (12) is the second half of the equations of motion of a rigid body. Their left sides are obtained from the solution of Euler's equations. Thus, they become three coupled differential equations for the Euler angles which gives the orientation of the body as a function of time. In this simulation, the equations of motion from eqn. (10) are used to calculate the angular velocity and position. The model for the plant dynamics is given in Appendix A, Fig. A4.

4. SPACECRAFT CONTROL MODES

4.1 Introduction to spacecraft attitude control

Attitude control is the process of achieving and maintaining an orientation in space. Attitude control systems consist of a set of control system hardware, such as attitude sensors that locate known reference targets like the Sun or the Earth to determine the attitude. The actuator is selected based on the mission requirements, receives control commands and issues the control torque.

The output of a SC attitude control system is the measured position, θ_m , and feedback is used to obtain an error signal such that $\theta = \theta_{ref} - \theta_m$. The error signal is used to generate a control torque to counter the effect of the input disturbance torque and control the output θ_m near θ_{ref} . A common method for the spacecraft attitude controller is a position-plus-rate control law. An example of a pitch-axis attitude control system is given in Fig. 2. The control torque, N_c , is directly proportional to the error signal and its time derivative.

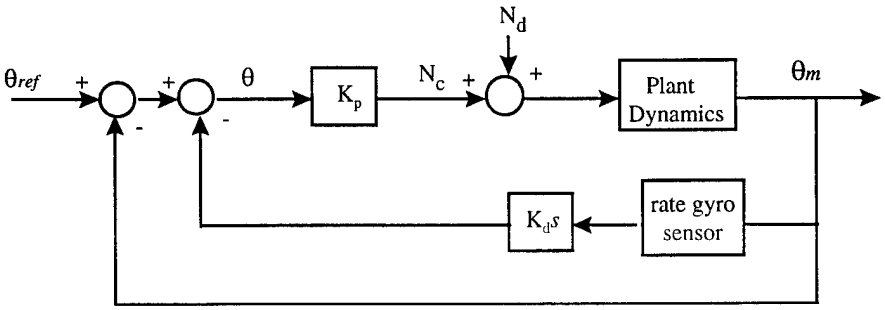

Fig. 2. Position-plus-rate pitch control system.

4.2 Backup control mode

The most common passive control techniques are *spin stabilization*, in which the entire spacecraft is rotated so that its angular momentum vector remains approximately fixed in inertial space and *gravity-gradient stabilization*, in which the differential gravitational forces acting on an asymmetric spacecraft force the minor axis to be perpendicular to the gravitational equipotential. Passive control normally requires the use of mass expulsion jets or magnetic coils to occasionally adjust the spacecraft attitude and spin rate to counteract disturbance torques. In addition, some form of nutation damping is required to eliminate nutation caused by an unbalanced spacecraft.

Normally, spin-stabilized spacecraft spin about the major principle axis for stability.[8] The requirements for spin stabilization is

$$\left|\int \mathbf{N}dt\right| << |\mathbf{L}| \tag{12}$$

where **L** is the spacecraft angular momentum, **N** is the sum of the disturbance torques. The integral defines the change in both the orientation and the spin rate. If the disturbance torques have significant trends which exceed the mission attitude constraints, an active control system is used to adjust the attitude and the spin rate.

5. SIMULATION RESULTS

In this feedback representation of the system (see Fig. 3), the angular position is a function of the sensor input. This example shows sensor activation with respect to one axis of rotation. The simulated controller output is compared to measured data. In this development, the essential dynamics in the system are modeled as an example of the neural controller in a dynamic system and show that there is a qualitative agreement between the simulation and the angular specifications for backup control mode on a low earth orbit satellite[4]. The subsystem modules are contained in Appendix A.

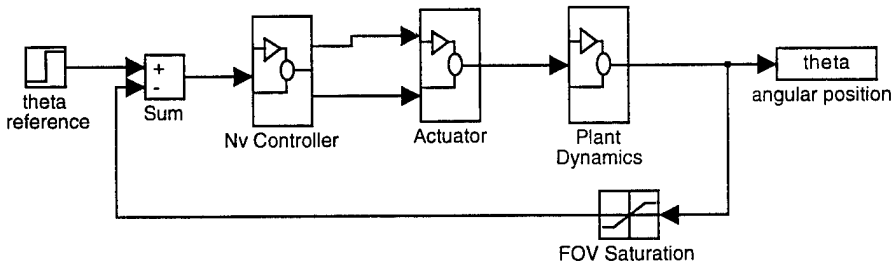

Fig. 3 System Block Diagram

5.1 Controller results

An oscillator is constructed by connecting the neurons in series. The sensor input, time-series data, to each neuron changes the frequency of the oscillator. The angular position error is filtered with a phase lead network to provide damping. The output of the neurons is a push-pull configuration. Therefore, the neuron output is summed and the voltage across the load, the control output signal, is either plus or minus the rail voltage. The controller subsystem is shown in Appendix A, Fig. A2.

To demonstrate how the controller responds to sensor inputs, two cases are examined; the sensor inputs to the neurons are equal and constant (Fig. 4); and the sensor inputs are not equal (i.e. one sensor is activated, Fig. 5). In the first case for ambient conditions, the sensor input to each neuron is a constant simulating the neuron input bias when the sensors are activated via sunlight. In Fig. 5, the sensor input of one neuron is decreased and the duty cycle across the activated neuron is decreased, indicative of the FOV of the sensor being out of range of the Sun. It is crucial to determine the frequency of oscillation for the network in the system as a faster oscillator will yield no output control torque. A slowly varying sinusoidal input is used as the input reference and the results are given in Fig. 6. It is interesting to note that since the input amplitude does not vary greatly, (stays within an amplitude of one) the neuron output signal does not change significantly. This is an important point, in that one can introduce a sinusoid or random noise at the input of the neuron and maintain the oscillation frequency of the network as seen in the output control signal.

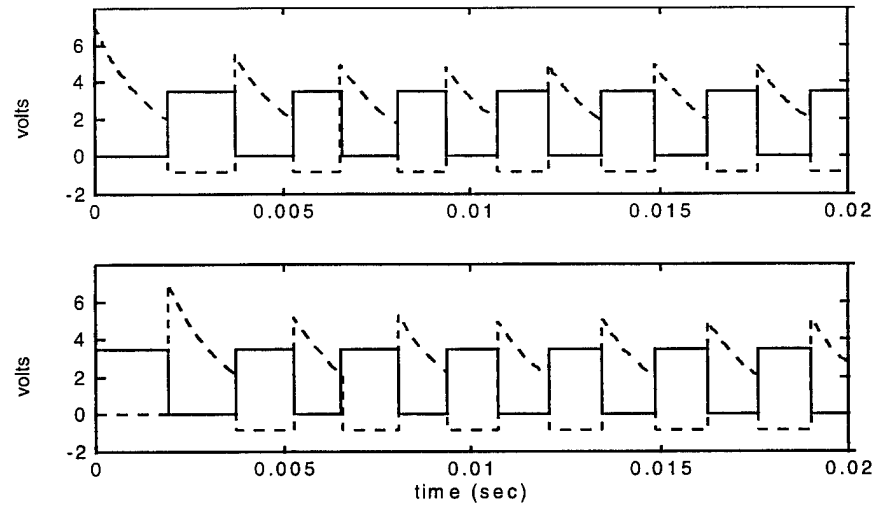

Fig. 4. Simulated input (dashed) to the neuron and output (solid pulse for the network with a constant input bias, $\tau = .003$ sec.

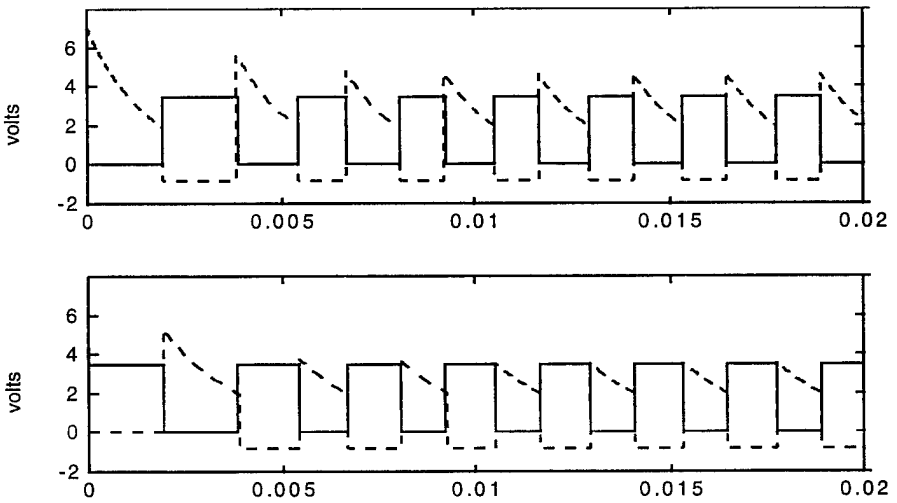

Fig. 5. Simulated input (dashed) to the neuron and output (solid) pulse for the network with one sensor input activated (bottom), $\tau = .003$ sec.

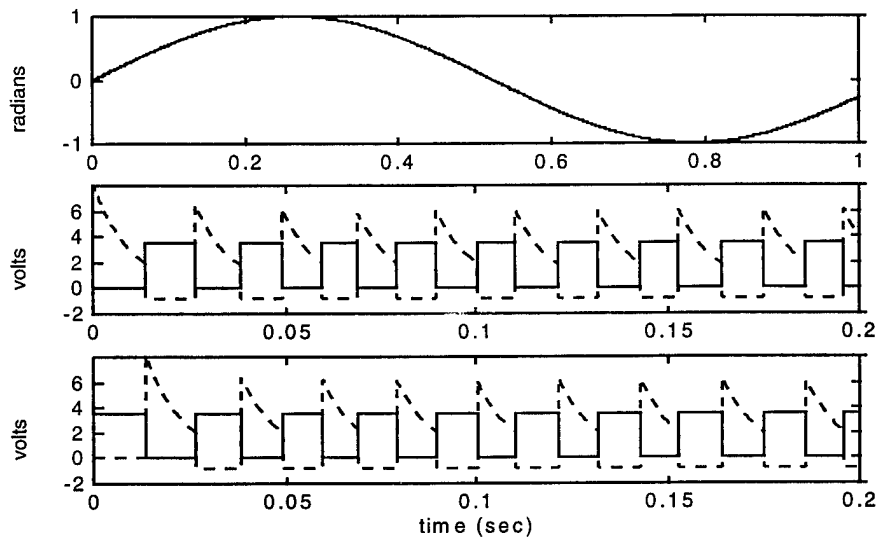

Fig. 6. Simulated neuron input (dashed) and output (solid) pulse for the network with sinusoid inputs of 1 radian/second (top).

5.2 Angular position results

The results of the simulation for two different angles are shown in Fig. 7 and Fig. 8. For the stationary position, $\theta = 0$ degrees and small angles, $\theta = 1$ degree, some overshoot in the angular position is expected, but the response reaches steady state. These results demonstrate the effect of using the lead filter in reducing overshoot and improving convergence. On FORTE the backup control mode, using gravity gradient stabilization with magnetic control suggests an accuracy of more than one degree for the pitch and roll axes[4], and the attitude error does not show asymptotic convergence. The use of magnetic torque coils contributes to the inaccuracy.[8] Comparatively, the results of this system for small angular corrections, show the system response would suffice per the specifications on a low earth orbit backup control mode.

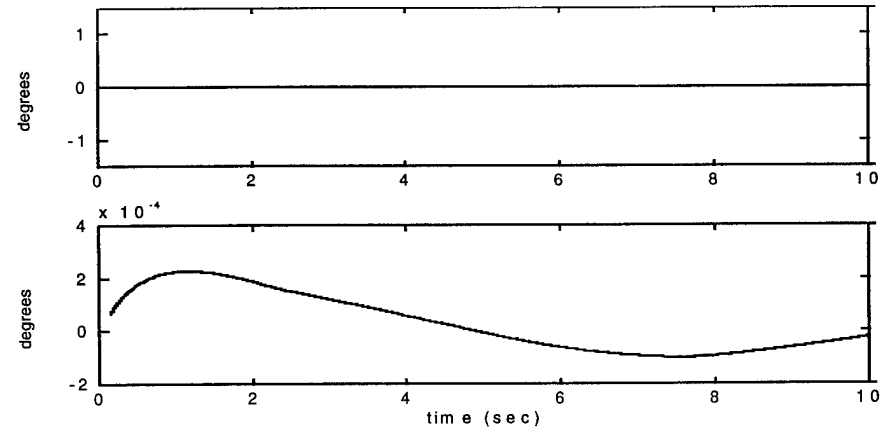

Fig. 7. Angular Position output for a constant step input, $\theta = 0$ degree.

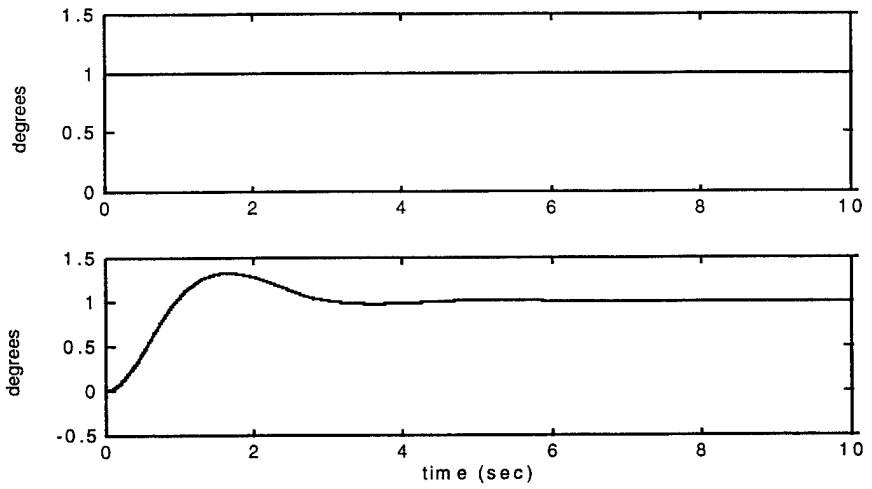

Fig. 8. Angular Position output for a constant step input, $\theta = 1$ degree.

6. CONCULSIONS

These oscillators could be constructed for multiple axis control with sensory input from analog sun sensors. The changes in input intensity of the sensors cause motion toward the Sun or vise versa. Further, the FOV of the sensor will indicate an off-nominal position on an axis and activate the controller to move accordingly. The results of the angular position simulation give some evidence to support further investigation of this controller in SC control systems, especially for control modes where the pointing accuracies are not extremely small. Use of this control method, in future spacecraft control systems may improve reliability during the spacecraft mission by adding a degree of autonomy to the vehicle.

7. REFERENCES

[1]Warner, Richard, "Magnetic Control of Spacecraft Attitude," ISSO, pp. 5-7, December, 1993.

[2]Psiaki, Mark L., Huang, Lejin, "Ground Tests of Magnetometer-Based Autonomous Navigation (MAGNAV) for Low-Earth-Orbiting Spacecraft," Journal of Guidance, Control, and Dynamics, Vol. 16, No. 1, pp. 206-214, Jan.-Feb. 1993.

[3]Tai, F., and Noerdlinger, P. D., "A Low Cost Autonomous Navigation System," Guidance and Control 1989, Proceedings of the Annual Rocky Mountain Guidance and Control Conference, American Astronautical Society, San Diego, pp. 3-23, 1989.

[4]Fox, S. M. and Pal, P. K., " An Attitude Control and Determination Subsystem For the Fast On-Orbit Recording of transient Events Satellite," AAS/AIAA Spaceflight Mechanics Meeting, AAS Publishing, San Diego, 1995.

[5] Wasserman, Philip D., "*Neural Computing Theory and Practice*," Chp. 1-2, Van Hostrand Reinhold, New York, 1989.

[6] Hasslacher, B., and Tilden, Mark W., "Living Machines," Robotics and Autonomous System: The Biology and Technology of Intelligent Autonomous Agents, Elsivier Publishers, Spring 1995.

[7] Braitenberg, Valentino, *Vehicles Experiments in Synthetic Psychology*, Chp. 2-5, MIT Press, Cambridge, 1984.

[8]Wertz, James R., *Spacecraft Attitude Determination and Control*, Chp. 6 and 19, Kluwer Academic Publishers, Dordrecht, 1978.

[9]Priedhorsky, William C., "The ALEXIS Small Satellite Project: Initial Flight Results," *SPIE Proceedings*, Vol. 2006, pp. 114-127, Bellingham, 1993.

[10]Wiesel, William E., *Spaceflight Dynamics*, Chp. 4 and 5, McGraw-Hill, Inc., New York, 1989.

[11]Chobotov, V. A., *Spacecraft Attitude Dynamics and Control*, Chp. 8, Krieger Publishing Co., Malabar, 1991.

8. APPENDIX A

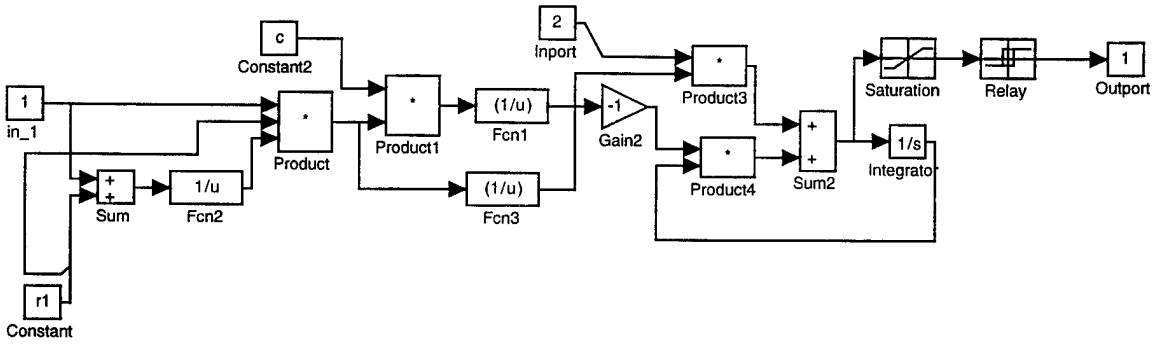

Fig. A1. Neuron Model

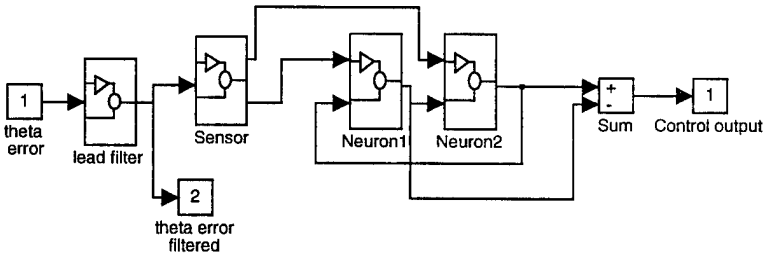

Fig. A2. Controller Model

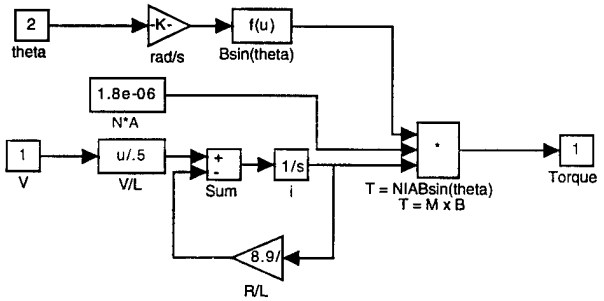

Fig. A3. Actuator Model

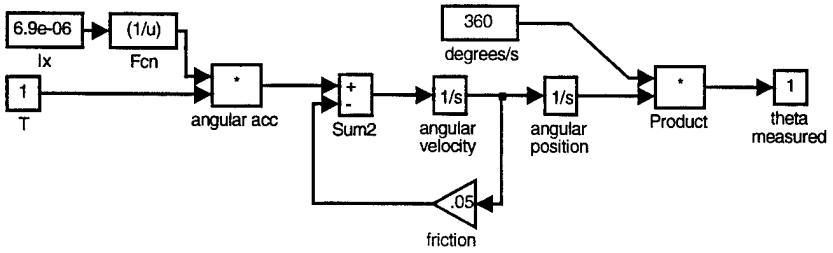

Fig. A4. Plant Dynamics

Report Number (14) LA-UR--97-4334
CONF-971086--

Publ. Date (11) 199803
Sponsor Code (18) DOE/DP, XF
UC Category (19) UC-700, DOE/ER

DOE